Applied Radiation and Isotopes 225 (2025) 112088

Contents lists available at ScienceDirect

Applied Radiation and Isotopes

journal homepage: www.elsevier.com/locate/apradiso

# New cross sections for $^{165}$Ho($p,x$) reactions focused on production of a perspective Auger electron emitter $^{165}$Er

Jaroslav Červenák, Kateřina Ondrák Fialová, Lukáš Ondrák, Ondřej Lebeda *

*Nuclear Physics Institute of the Czech Academy of Sciences, Czech Republic*

ARTICLE INFO

*Keywords:*
Cross-sections
Excitation functions
$^{165}$Er
$^{164m,g}$Ho
Auger electron therapy

ABSTRACT

Erbium-165 is pure Auger electron emitter and promising candidate for targeted radionuclide therapy. Investigation of its production routes is therefore highly desirable. Only a few cross-section measurements of its production via the $^{165}$Ho($p,n$) nuclear reaction are available, and the data are not entirely consistent.

In this work, we present new cross-section measurements of the $^{165}$Ho($p,n$)$^{165}$Er reaction and the $^{165}$Ho($p,x$)$^{164m,g}$Ho side reactions covering the proton energy range up to 20 MeV. The obtained data are compared to previously published data as well as to the prediction of the nuclear reaction model code TALYS 1.96. Thick target yields deduced from the measured cross sections confirm feasibility of $^{165}$Er production in clinically relevant amounts and high radionuclidic purity. The investigated production route is particularly suitable for implementation on common small cyclotrons and deserves further development.

## 1. Introduction

Erbium-165 ($T_{½}$ = 10.36 h, EC = 100 %) is the next rare-earth element (REE) with promise in medicine. It undergoes electron capture, which is followed by the emission of Auger electrons with energies of 5.33 and 38.4 keV, in addition to several low-energy X-rays with energies ranging from 6.72 to 55.30 keV. These decay properties make $^{165}$Er a suitable candidate for single-photon emission computed tomography (SPECT), but mainly for targeted radionuclide therapy (TRNT).

Erbium-165 is not the first REE attractive for TRNT. The most widely used REEs in TRNT are, naturally, those with proper decay characteristics and production routes that yield sufficient activities for clinical applications, such as $^{90}$Y, $^{153}$Sm or $^{177}$Lu with the emission of β particles (Parus and Mikolajczak, 2012; Civelek and Wong, 2021; Song and Sgouros, 2024). However, even among the Auger electron emitters, $^{165}$Er is not the first REE investigated for use in TRNT. $^{161}$Tb has been recently investigated in detail due to its potential to outperform $^{177}$Lu (Lehenberger et al., 2011; Alcocer-Ávila et al., 2020).

Radionuclides emitting β particles have been shown to be effective in the treatment of large and solid tumours, such as neuroendocrine or prostate cancer, due to the range and suitable linear energy transfer (LET) of the emitted β particles (Strosberg et al., 2017). In contrast, Auger emitters may find their application in the therapy of small or micrometastatic tumours due to the short-range high LET electrons they emit (Aghevlian et al., 2017).

There are several routes of production of $^{165}$Er via charged-particle induced reactions. The most favourable seems to be the direct route to $^{165}$Er by bombardment of Ho targets with protons or deuterons due to the fact that holmium is naturally monoisotopic element:

$$^{165}\text{Ho}(p,n)^{165}\text{Er} \quad (1)$$

$$^{165}\text{Ho}(d,2n)^{165}\text{Er} \quad (2)$$

Reaction 1 seems to be the most promising because the proton energies needed for maximal yield fall into the range of widespread small cyclotrons ($E_p \leq 18$ MeV). The maximal cross section for Reaction 1 was determined experimentally (166–180 mb) for proton energies of 9.5–11.3 MeV (Gracheva et al., 2020; Tárkányi et al., 2008a; Beyer et al., 2004). Reaction 2 was also investigated and its maximum was found near 600 mb for deuteron energies 12.4–13.6 MeV (Tárkányi et al., 2008b; Hermanne et al., 2013). Predictions based on the nuclear reaction model code TALYS-1.2 for Reaction 2 were even higher, 754 mb at 13 MeV (Sadeghi, 2010).

The indirect route via the short-lived $^{165}$Tm ($T_{½}$ = 1.25 d, EC = 100 %) through activation of two erbium stable isotopes ($^{164}$Er and $^{166}$Er) is another option:

$$^{166}\text{Er}(p,2n)^{165}\text{Tm} \rightarrow ^{165}\text{Er} \quad (3)$$

* Corresponding author.
*E-mail address:* lebeda@ujf.cas.cz (O. Lebeda).

https://doi.org/10.1016/j.apradiso.2025.112088
Received 1 July 2025; Received in revised form 3 August 2025; Accepted 6 August 2025
Available online 6 August 2025

$^{166}$Er($d$,3$n$)$^{165}$Tm→$^{165}$Er (4)

$^{164}$Er($d$,$n$)$^{165}$Tm→$^{165}$Er (5)

The predicted maxima of Reactions 3 and 4 are large, 1260 mb and 1525 mb at 21 MeV and 25 MeV, respectively. In contrast, Reaction 5 does not seem to be of interest for production of $^{165}$Er, because the predicted shape and maximum of the excitation function indicates a small yield. It however contributes to the formation of $^{165}$Er in deuteron irradiation of $^{nat}$Er targets (Sadeghi, 2010).

We therefore decided to investigate excitation functions of proton-induced reactions on $^{165}$Ho and to compare them with the previous measurements and current prediction of TALYS 1.96 (Koning et al., 2023). Cross-sections of the $^{165}$Ho($p$,$n$)$^{165}$Er reaction were re-measured together with the simultaneously running reaction $^{165}$Ho($p$,$x$)$^{164m,g}$Ho. Thick target yields deduced from the obtained data allowed us to estimate the potential of this $^{165}$Er production route.

## 2. Materials and methods

### 2.1. Target and irradiation

One stack of foils containing 12 Ho targets (99.9 %, 8.84–11.25 μm thick, GoodGellow), 12 Ti monitors (99.6 %, 11.43 μm thick, AlfaAesar), several Cu degraders (55.9 and/or 10.6 μm thick, GoodFellow), and a Ag beam stop was irradiated on the external proton beam line of the cyclotron U-120M at the Nuclear Physics Institute of the CAS. The precise thicknesses of the foils and their uncertainties were calculated after weighing the foils prior to the irradiation. The stack was placed in a Faraday-cup-like holder. The beam energy loss and straggling were calculated with SRIM2008 (Ziegler et al., 2008). The incident proton energy determined from the measurement of the beam orbit position was 19.95 ± 0.20 MeV. Beam current was recorded each second of the irradiation and integrated over the bombardment time, $t_b$. The beam parameters were confirmed by re-measurement of the beam monitoring reaction $^{nat}$Ti($p$,$x$)$^{48}$V excitation function and its comparison with recommended data (Červenák and Lebeda, 2020; Hermanne et al., 2018).

### 2.2. Activity measurement and cross-section calculation

After the end of bombardment (EOB), single foils were measured on three energy- and efficiency-calibrated γ-ray spectrometers equipped with HPGe detectors: two coaxial GEM40P4-83-SMP (Ortec) and GC4018 (Canberra), as well as one planar GL0515R (Canberra). The calibration was performed using a set of standards ($^{241}$Am, $^{152}$Eu, $^{133}$Ba) provided by the Czech Institute of Metrology with combined standard uncertainties varying from 0.4 % to 1.0 %. Detection efficiency curves were measured for each sample-to-detector distance.

Gamma-ray spectra were evaluated manually using the standard Canberra program GENIE2K with interactive peak fitting utility. Net peak areas of the γ lines used for quantification of a given radionuclide were corrected for their mean attenuation in the foils as well as for the attenuation in the polyethylene bag in which they were measured.

The decay data used for the activity calculation were adopted from the NuDat3 database (NuDat 3.0, NNDC), originally published in Nuclear Data Sheets (Singh and Chen, 2018, 2024). $Q$-values and thresholds of the reactions were calculated via $Q$-calc program online (Pritychenko and Sonzogni, NNDC). The decay and nuclear reaction data relevant for the experiment are summarized in Table 1.

Cross-sections were calculated using the activation formula (equation (6)):

$$\sigma = \frac{P_\gamma}{I_\gamma \eta t_m} \frac{\lambda t_r}{1 - e^{-\lambda t_r}} e^{\lambda t_c} \frac{Aze}{d\rho N_A I (1 - e^{-\lambda t_b})}, \quad (6)$$

where $\sigma$ is cross-section for formation of the radionuclide at the energy in the middle of the foil (cm$^2$), $P_\gamma$ is net peak area of the γ line used for the quantification of radionuclide, $I_\gamma$ is intensity of this γ line, $\eta$ is detection efficiency for this γ line, $t_m$ is live time of the measurement (s), $t_r$ is real time of measurement (including the dead time) (s), $t_c$ is time between the EOB and the start of the measurement (s), $A$ is atomic weight of the foil's metal (g/mol), $z$ is proton charge (z = 1), $e$ is elementary charge (1.602177 × 10$^{-19}$ C), $d$ is foil's thickness (cm), $\rho$ is density of the foil's metal (g/cm$^3$), $N_A$ is Avogadro's number (6.022137 × 10$^{23}$ mol$^{-1}$), $I$ is beam current (A), $\lambda$ is decay constant of the radionuclide (s$^{-1}$), and $t_b$ is irradiation time (s).

Total cross-section uncertainty was deduced from partial uncertainties of the parameters in the activation formula summarized below:

- detection efficiency for a γ line selected for activity calculation (<3 %)
- emission probability of a γ line selected for activity calculation (usually <5 %)
- net peak area of a γ line selected for activity calculation (<10 %)
- beam current (5 %)
- thickness of the foil (<2 %)

After the evaluation of cross-sections, the excitation functions were compared with previously published experimental data and with theoretical predictions of the TALYS 1.96 nuclear reaction model code (Koning et al., 2023).

## 3. Results and discussion

### 3.1. Beam energy and current

The proton current recorded by the beam integrator was 0.932 μA. The remeasured excitation function of the beam monitoring reaction using the incident beam energy and the beam current is displayed in Fig. 1. The measured cross sections agree very well with the recommended data (Červenák and Lebeda, 2020; Hermanne et al., 2018).

**Table 1**
Decay data of the investigated radionuclides and nuclear reactions, in which they are formed. $Q$-values for isomeric nuclei need to be lowered by the energy level of the isomer. $Q$-values and threshold energies for reactions in which composed particles are emitted are to be increased by binding energy of the particle ($d = pn + 2.225$ MeV). Energies and intensities of γ lines used for quantification are in bold, uncertainties are in italics.

| RN | T½ | $E_\gamma$ (keV) | $I_\gamma$ (%) | reaction | $Q$ (MeV) | $E_{thr}$ (MeV) |
|---|---|---|---|---|---|---|
| $^{165}$Er | 10.36 h *4* | 46.7 | 21.5 *5* | $^{165}$Ho($p$,$n$)$^{165}$Er | −1.1590 *12* | 1.1661 *12* |
| | | 47.547 | 37.9 *8* | | | |
| | | **53.695**[a] | **3.99 *8*** | | | |
| | | **53.877**[a] | **7.73 *16*** | | | |
| | | 55.293 | 2.59 *6* | | | |
| $^{164g}$Ho | 28.8 min *4* | **91.39 *3*** | **2.3** | $^{165}$Ho($p$,$pn$)$^{164}$Ho | −7.9888 *16* | 8.0376 *16* |
| | | 73.392 *5* | 1.88 | | | |
| $^{164m}$Ho | 36.6 min *3* | **56.64 *5*** | **6.5 *3*** | | | |

[a] Sum of these two unresolved peaks and their intensities was used for calculations.

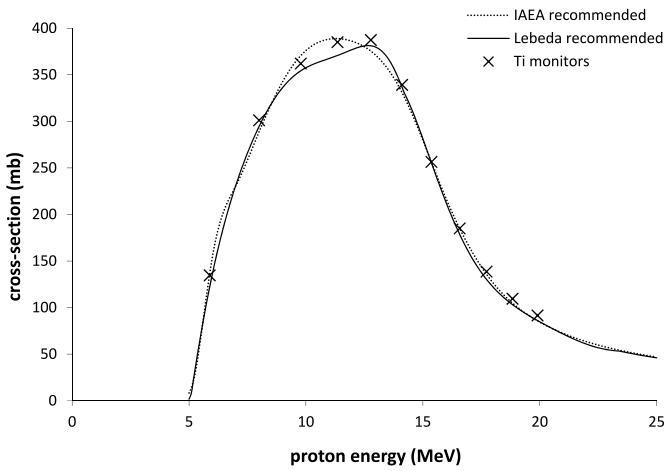


**Fig. 1.** Re-measurement of the monitoring reaction $^{nat}$Ti($p,x$)$^{48}$V.

### 3.2. Cross sections

The cross sections measured in this work are summarized in Table 2. They are also shown in Figs. 2–4 together with the previously published experimental data and with the prediction of the TALYS 1.96 nuclear reaction model code using its default parameters (Koning et al., 2023).

#### 3.2.1. Cross-sections for $^{165}$Ho($p,n$)$^{165}$Er reactions

The activity of $^{165}$Er has been calculated after complete decay of $^{163}$Er using its X-rays with energies 46.70 keV, 47.55 keV, and 53.79 keV with respective intensities of 21.5 %, 37.9 % and 11.72 % (the latter being the sum of 53.70 keV and 53.88 keV X-rays with intensities of 3.99 % and 7.73 % respectively). Activities and cross sections calculated using different X-rays provided consistent results. We used the sum of 53.70 and 53.88 keV X-rays for calculation the cross sections presented in Table 2 and in Fig. 2. Our data are in a good agreement with the data of Gracheva et al. (2020) and Tárkányi et al. (2008a) even though the peak of our excitation function seems to be narrower, sharper and its amplitude slightly lower. The data of Beyer et al. (2004) seem to be systematically shifted towards higher energies by 1.5–2 MeV, but corresponds well in shape and amplitude with other experimental data. Recommended cross sections obtained as PADÉ fit of the experimental data in Tárkányi et al. (2024) agree within uncertainties with our measurement, which indicates slightly lower values for $E_p > 9$ MeV.

The TALYS 1.96 prediction reproduces well the shape of the experimental data, but the excitation function maximum is shifted to lower energies by ca. 1.5 MeV, and the cross sections seem to be underestimated in the energy interval of 8.5–14 MeV.

**Table 2**
Measured isotopic cross sections for the formation of $^{165}$Er, $^{164m}$Ho and $^{164g}$Ho in proton-induced nuclear reactions on $^{165}$Ho. The cross sections for direct formation of $^{164g}$Ho were deduced after subtraction of the $^{165m}$Ho decay contribution to the $^{164g}$Ho activity, if possible.

| $E_p$ (MeV) | $\sigma$ (mb) | | |
|---|---|---|---|
| | $^{165}$Er | $^{164m}$Ho | $^{164g}$Ho |
| 19.80 ± 0.20 | 31.2 ± 2.0 | 33.0 ± 2.3 | |
| 18.73 ± 0.21 | 32.3 ± 2.1 | 23.2 ± 1.6 | |
| 17.61 ± 0.22 | 33.9 ± 2.2 | 13.9 ± 1.0 | 9.2 ± 1.8 |
| 16.46 ± 0.23 | 36.5 ± 2.4 | 8.71 ± 0.60 | 5.9 ± 1.0 |
| 15.25 ± 0.24 | 42.3 ± 2.7 | 4.38 ± 0.31 | 3.21 ± 0.53 |
| 13.99 ± 0.26 | 54.2 ± 3.5 | 1.86 ± 0.14 | 0.62 ± 0.24 |
| 12.65 ± 0.27 | 81.1 ± 5.2 | 0.499 ± 0.054 | |
| 11.22 ± 0.31 | 122 ± 7.9 | | |
| 9.63 ± 0.35 | 149 ± 9.7 | | |
| 7.82 ± 0.39 | 81.5 ± 5.3 | | |
| 5.66 ± 0.49 | 8.67 ± 0.57 | | |
| 3.87 ± 0.69 | 0.537 ± 0.036 | | |

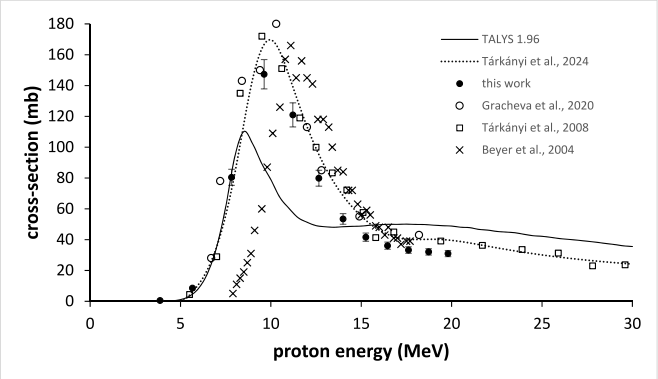


**Fig. 2.** Cross sections of the $^{165}$Ho($p,n$)$^{165}$Er reaction in comparison with previously measured data and their PADÉ fit (recommended cross sections available at www-nds.iaea.org/medical), as well as with the prediction of the nuclear reaction model code TALYS 1.96 (default parameters).

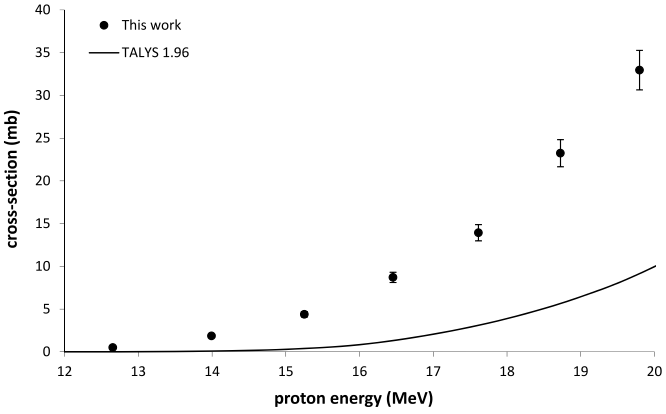


**Fig. 3.** Cross sections of the $^{165}$Ho($p,x$)$^{164m}$Ho reaction in comparison with prediction of the nuclear reaction model code TALYS 1.96 (default parameters).

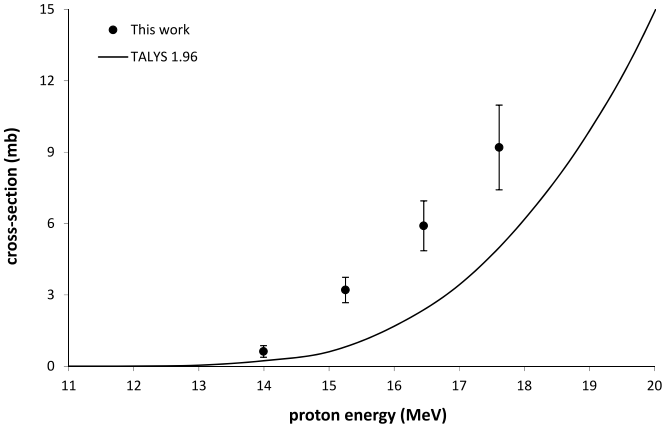


**Fig. 4.** Cross sections of the $^{165}$Ho($p,x$)$^{164g}$Ho reaction in comparison with prediction of the nuclear reaction model code TALYS 1.96 (default parameters).

#### 3.2.2. Cross-sections for $^{165}$Ho($p,x$)$^{164m,g}$Ho reactions

The isomers $^{164m,g}$Ho can be produced solely in the reactions $^{165}$Ho($p,pn$) and $^{165}$Ho($p,d$). They have comparable half-lives, and the ground state is continuously fed by isomeric transition of $^{164m}$Ho. The activity of $^{164m}$Ho was calculated using its 56.64 keV γ line with intensity of 6.5 %

and the activity of $^{164g}$Ho was calculated using its 91.39 keV γ line with intensity of 2.3 %. The activity of the ground state was corrected for the contribution of the activity born from $^{164m}$Ho during and after irradiation. For detailed description of the correction, we refer to our previous work (Lebeda and Pruszyński, 2010). Due to the short half-lives of both isomers and delay in the subsequent foils' measurement, not all the spectra could be used for deducing independent cross sections for the $^{164g}$Ho formation. The results are displayed in Figs. 3 and 4. It is the first measurement of the cross sections for the $^{165}$Ho($p,x$)$^{164m,g}$Ho reactions. We may, therefore, compare our data only to the theoretical prediction of TALYS 1.96. It reproduces well the trend of our measurement, but it markedly underestimates the absolute values—around 20 MeV, our cross sections are ca. four times larger than the predictions for $^{164m}$Ho and ca. twice lower for $^{164g}$Ho.

### 3.3. Thick target yields

The thick target yield for production of $^{165}$Er was calculated from the measured cross sections fitted with two polynomials by integrating them with use of the proton stopping power in holmium. The result is displayed in Fig. 5 together with the only available measured thick target yield point measured by Gracheva et al. (2020). This point agrees with the curve deduced from the cross sections measured in this work within the uncertainties, which are relatively large in this particular case.

Production of $^{165}$Er with high radionuclidic purity is readily achievable via the $^{165}$Ho($p,n$) reaction, because there is no other radioisotope of erbium produced in the target in the beam energy range of 5–15 MeV. The only other radionuclides produced in the target in this energy interval are the isomers $^{164m,g}$Ho, whose amount in the target will be relatively small. They also decay much faster than $^{165}$Er and will likely be chemically separated from the product together with the target matrix.

For potential production of $^{165}$Er, the proton energy loss 15 → 5 MeV seems to be optimal. The target thickness necessary for such beam energy loss deduced from proton stopping powers in holmium obtained from SRIM2008 is 0.58 mm (Ziegler et al., 2008). The EOB activities for increasing bombardment time, our suggested beam energy loss, and the fixed beam current of 50 μA are summarized in Table 3.

Five-hour long bombardment forms 138 GBq of $^{165}$Er at EOB, and doubling the irradiation time increases the EOB activity to 236 GBq. Even taking into account decay during a complex separation process, which may take up to 5 h as described in (Bolcaen et al., 2023; Da Silva et al., 2021), it is a more than acceptable production yield from many viewpoints such as target and beam price.

As no Auger electron emitters have yet been approved for clinical practice, it isn't straightforward to estimate the single patient dose. The most advanced investigated Auger electron emitter similar to $^{165}$Er is perhaps $^{161}$Tb ($T_{½}$ = 6.96 d; $\beta^-$ = 100 %). This radionuclide has similar chemical properties and average number of Auger electrons emitted per decay (10.9 for $^{161}$Tb and 7.2 for $^{165}$Er), however, it emits also β electrons (Verburg et al., 2023). Some preliminary studies showed that in case of $^{161}$Tb, the applied therapeutic activities could be lower compared to clinically established $\beta^-$ emitter $^{177}$Lu, when targeting similar tissues such as neuroendocrine tumours or prostate cancer due to higher therapeutic efficiency of Auger electrons emitted (Verburg et al., 2023; Baum et al., 2021; Müller et al., 2023). Some studies suggest activities of up to 5.4 GBq of $^{161}$Tb per therapy cycle (Verburg et al., 2023), which could potentially apply for $^{165}$Er as well. This activity is readily achievable via the $^{165}$Ho($p,n$)$^{165}$Er route investigated here. Taken together with other aspects discussed above, the studied production route of $^{165}$Er via $^{165}$Ho($p,n$)$^{165}$Er reaction feasibly enables further exploration of this promising radionuclide in nuclear medicine.

## 4. Conclusion

In this work, we present newly measured data for excitation functions of reactions relevant to the production of $^{165}$Er, $^{164m}$Ho, and $^{164g}$Ho. The latter two reactions' functions are reported for the first time.

In discussion of thick target yields, we demonstrate that the reaction $^{165}$Ho($p,n$)$^{165}$Er is applicable to $^{165}$Er production scale estimated for early human studies (based on the assumption of similar activities to $^{161}$Tb-labeled therapeutic drugs) with high radionuclidic purity.

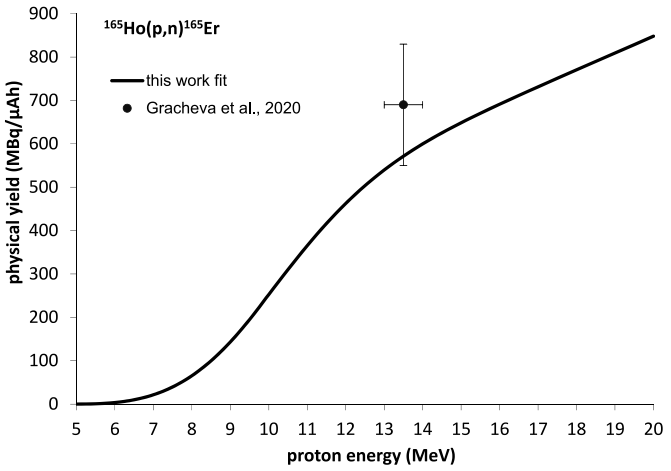


**Fig. 5.** Thick target yield of $^{165}$Er in the $^{165}$Ho($p,n$)$^{165}$Er reaction calculated from the cross sections measured in this work (cf. Table 2) and beam energy leaving the target equal to 5 MeV. Experimental thick target yield at 13.5 MeV measured in Gracheva et al. (2020) is displayed for comparison as well.

**Table 3**
EOB activities of $^{165}$Er produced in a thick target for increasing bombardment time $t_b$ (beam energy loss $\Delta E_p$ = 15 → 5 MeV, beam current $I$ = 50 μA, physical yield $Y$ = 648.5 MBq/μAh).

| $t_b$ (h) | $A_{EOB}$ (GBq) |
|---|---|
| 2.5 | 75 |
| 5 | 138 |
| 7.5 | 191 |
| 10 | 236 |

## CRediT authorship contribution statement

**Jaroslav Červenák:** Writing – review & editing, Writing – original draft, Investigation, Formal analysis, Data curation, Conceptualization. **Kateřina Ondrák Fialová:** Writing – review & editing, Writing – original draft, Investigation, Formal analysis, Data curation, Conceptualization. **Lukáš Ondrák:** Writing – review & editing, Writing – original draft, Investigation, Formal analysis, Data curation, Conceptualization. **Ondřej Lebeda:** Writing – review & editing, Supervision, Project administration, Methodology, Investigation, Funding acquisition, Formal analysis, Data curation.

## Declaration of competing interest

The authors declare that they have no known competing financial interests or personal relationships that could have appeared to influence the work reported in this paper.

## Acknowledgements

The authors are grateful to Ing. Jan Štursa and the crew of the U-120M cyclotron for the irradiations, to Dr. Jan Kameník for the help with γ-ray spectra measurement and to Dr. J.W. Engle for a thorough revision of the manuscript. The work was performed on the infrastructures

CANAM supported by the research plan RVO61389005 of the Nuclear Physics Institute of the Czech Academy of Sciences, and EATRIS-CZ supported by the infrastructural project LM2023053 of the Ministry of Education, Youth and Sports.

## Data availability

Data will be made available on request.

## References


Aghevlian, S., Boyle, A.J., Reilly, R.M., 2017. Radioimmunotherapy of cancer with high linear energy transfer (LET) radiation delivered by radionuclides emitting α-particles or Auger electrons. Adv. Drug Deliv. Rev. 109, 102–118. https://doi.org/10.1016/j.addr.2015.12.003.

Alcocer-Ávila, M.E., Ferreira, A., Quinto, M.A., Morgat, C., Hindié, E., Chmpion, C., 2020. Radiation doses from $^{161}$Tb and $^{177}$Lu in single tumour cells and micrometastases. EJNMMI Phys 7, 1–9. https://doi.org/10.1186/s40658-020-00301-2.

Baum, R.P., Singh, A., Kulkarni, H.R., Bernhardt, P., Rydén, T., Schuchardt, C., Gracheva, N., Grundler, P.V., Köster, U., Müller, D., Pröhl, M., Zeevaart, J.R., Schibli, R., van der Meulen, N.P., Müller, C., 2021. First-in-Humans application of $^{161}$Tb: A Feasibility Saufy Using $^{161}$Tb-DOTuTOC. J. Nucl. Med. 62, 1391–1397. https://doi.org/10.2967/jnumed.120.258376.

Beyer, G.J., Zeisler, S.K., Becker, D.W., 2004. The Auger-electron emitter $^{165}$Er: excitation function of the $^{165}$Ho(p,n)$^{165}$Er process. Radiochim. Acta 92, 219–222. https://doi.org/10.1524/ract.92.4.219.35608.

Bolcaen, J., Gizawy, M.A., Terry, S.Y.A., Paulo, A., Cornelissen, B., Korde, A., Engle, J., Radchenko, V., Howell, R.W., 2023. Marshalling the potential of Auger Electron radiopharmaceutical therapy. J. Nucl. Med. 64, 1344–1351. https://doi.org/10.2967/jnumed.122.265039.

Červenák, J., Lebeda, O., 2020. New cross-section data for proton-induced reactions on $^{nat}$Ti and $^{nat}$Cu with special regard to the beam monitoring. Nucl. Instrum. Methods Phys. Res. B 480, 78–97. https://doi.org/10.1016/j.nimb.2020.08.006.

Civelek, A.C., Wong, C.L., 2021. Radionuclide cancer therapy: unsealed alpha-and beta-emitters. In: Locoregional Radionuclide Cancer Therapy: Clinical and Scientific Aspects, pp. 61–87. ISBN 9783030562670.

Da Silva, I., Johnson, T.R., Mixdorf, J.C., Aluicio-Sarduy, E., Barnhart, T.E., Nickles, R.J., Engle, J.W., Ellison, P.A., 2021. A high separation factor for $^{165}$Er from Ho for Targeted Radiontclide Thrrapy. Molecutes 26, 7513. https://doi.org/10.3390/molecules26247513.

Gracheva, N., Carzaniga, T.S., Schibli, R., Braccini, S., vander Meulen, N.P., 2020. $^{165}$Er: a new candidate for Auger electron therapy and its possible cyclotron production from natural holmium targets. Appl. Radiat. Isot. 159, 109079. https://doi.org/10.1016/j.apradiso.2020.109079.

Hermanne, A., Adam-Rebeles, R., Tárkányi, F., Takacs, S., Csikai, J., Takacs, M.P., Ignatyuk, A., 2013. Deuteron induced reactions on Ho and La: experimental excitation functions and comparison with code results. Nucl. Instrum. Methods Phys. Res. B 311, 102–111. https://doi.org/10.1016/J.NIMB.2013.06.014.

Hermanne, A., Ignatyuk, A.V., Capote, R., Carlson, B.V., Engle, J.W., Kellett, M.A., Kibedi, T., Kim, G., Kondev, F.G., Hussain, M., Lebeda, O., Luca, A., Nagai, Y., Naik, H., Nichols, L.A., Nortier, F.M., Suryanarayana, S.V., Takacs, S., Tárkányi, F.T., Verpelli, M., 2018. Reference cross sections for charged-particle monitor reactions. Nucl. Data Sheets 148, 338–382. https://doi.org/10.1016/j.nds.2018.02.009. www-nds.iaea.org/medical/tip48v0.html.

Koning, A., Hilaire, S., Goriely, S., 2023. TALYS: modeling of nuclear reactions. Eur. Phys. J. A 59, 131. https://doi.org/10.1140/epja/s10050-023-01034-3. Available at http://nds.iaea.org/relnsd/talys/talys.html.

Lebeda, O., Pruszyński, M., 2010. New measurement of excitation functions for (p,x) reactions on $^{nat}$Mo with special regard to the formation of $^{95m}$Tc, $^{96m+g}$Tc, $^{99m}$Tc and $^{99}$Mo. Appl. Radiat. Isot. 68, 2355–2365. https://doi.org/10.1016/j.apradiso.2010.05.011.

Lehenberger, S., Barkhausen, C., Cohrs, S., Fischer, E., Grünberg, J., Hohn, A., Köster, U., Schibli, R., Türler, A., Zhernosekov, K., 2011. The low-energy $\beta^-$ and electron emitter $^{161}$Tb as an alternative to $^{177}$Lu for targeted radionuclide therapy. Nucl. Med. Biol. 38, 917–924. https://doi.org/10.1016/j.nucmedbio.2011.02.007.

Müller, C., van der Meulen, N.P., Schibli, R., 2023. Opportunities and potential challenges of using terbium-161 for targeted radionuclide therapy in clinics. Eur. J. Nucl. Med. Mol. Imag. 50, 3181–3184. https://doi.org/10.1007/s00259-023-06316-y.

NuDat 3.0. National Nuclear Data Center, information extracted from. https://www.nndc.bnl.gov/nudat/.

Parus, J., Mikolajczak, R., 2012. Beta-emitting radionuclides for peptide receptor radionuclide therapy. Curr. Top. Med. Chem. 12, 2686–2693. https://doi.org/10.2174/1568026611212230006.

Pritychenko, B., Sonzogni, A.. Q-value calculator, NNDC, Brookhaven National laboratory. Available at http://www.nndc.bnl.gov/qcalc.

Sadeghi, M., Enferadi, M., Tenreiro, C., 2010. Nuclear model calculations on the production of Auger emitter $^{165}$Er for targeted radionuclide therapy. J. Mod. Phys. 1, 217–225. https://doi.org/10.4236/jmp.2010.14033.

Singh, B., Chen, J., 2018. Nuclear data sheets for A=164. Nucl. Data Sheets 147, 1–381. https://doi.org/10.1016/j.nds.2018.01.001.

Singh, B., Chen, J., 2024. Nuclear structure and decay data for A=165 isobars. Nucl. Data Sheets 194, 460–877. https://doi.org/10.1016/j.nds.2024.02.003.

Song, H., Sgouros, G., 2024. Alpha and beta radiation for theragnostics. Pet. Clin. 19, 307–323. https://doi.org/10.1016/j.cpet.2024.03.006.

Strosberg, J., El-Haddad, G., Wolin, E., et al., 2017. Phase 3 trial of $^{177}$Lu-Dotatate for midgut neuroendocrine tumors. N. Engl. J. Med. 376, 125–135. https://doi.org/10.1056/NEJMoa1607427.

Tárkányi, F., Hermanne, A., Takács, S., Ditrói, F., Királyi, B., Kovalev, S.F., Ignatyuk, A.V., 2008a. Experimental study of the $^{165}$Ho(p,n) nuclear reaction for production of the therapeutic radioisotope $^{165}$Er. Nucl. Instrum. Methods Phys. Res. B 266, 3346–3352. https://doi.org/10.1016/J.NIMB.2008.05.123.

Tárkányi, F., Hermanne, A., Takács, S., Ditrói, F., Királyi, B., Kovalev, S.F., Ignatyuk, A.V., 2008b. Experimental study of the $^{165}$Ho (d,2n) and $^{165}$Ho (d,p) nuclear reactions up to 20 MeV for production of the therapeutic radioisotopes $^{165}$Er and $^{166g}$Ho. Nucl. Instrum. Methods Phys. Res. B 266, 3529–3534. https://doi.org/10.1016/J.NIMB.2008.05.123.

Tárkányi, F., Hermanne, A., Ignatyuk, A.V., Ditrói, F., Takács, S., Capote Noy, R., 2024. Extension of recommended cross section database for production of therapeutic isotopes. Radioanal. Nucl. Chem. 333, 717–804. https://doi.org/10.1007/s10967-023-09283-8 data available on. www-nds.iaea.org.

Verburg, F.A., de Blois, E., Koolen, S., Konijnenberg, M.W., 2023. Replacing Lu-177 with Tb-161 in DOTA-TATE and PSMA-617 therapy: potential dosimetric implications for activity selection. EJNMMI Phys 10, 69. https://doi.org/10.1186/s40658-023-00589-w.

Ziegler, J.F., Ziegler, M.D., Biersack, J.P., 2008. SRIM2008 code. Available at http://www.srim.org/.